A Comparison of MIMO-OFDM and MIMO-SCFDE in WLAN Environments

J. Coon, J. Siew, M. Beach, A. Nix, S. Armour, and J. McGeehan
Centre for Communications Research, University of Bristol
Merchant Venturers Building, Woodland Road, Bristol BS8 1UB, UK
Email: {Justin.Coon, Jiun.Siew}@bristol.ac.uk

***Abstract*— Recent developments in orthogonal frequency division multiplexing (OFDM) and single-carrier frequency-domain equalization (SCFDE) have sparked debate about the superiority of one method over the other. In this paper, we further this debate by comparing the theoretical performance of OFDM and SCFDE when each is implemented in one of two different multiple-input multiple-output (MIMO) architectures: spatial multiplexing and space-time block codes. This study focuses on the use of MIMO-OFDM and MIMO-SCFDE in wireless local area network (WLAN) applications. Performance is given in terms of the packet error rate (PER) and the throughput of the systems.**

I. Introduction

Lately, much attention has been focused on physical layer (PHY) techniques that are suitable for high-data-rate multiple-input multiple-output (MIMO) wireless communications systems. Of special interest are techniques that minimize the complexity of the multi-dimensional equalization process that is required in a wideband MIMO system. In this paper, we present arguments both for and against the use of two techniques, namely orthogonal frequency division multiplexing (OFDM) and single-carrier frequency-domain equalization (SCFDE). These arguments are presented in the form of a theoretical performance comparison.

In single-antenna systems, OFDM is well-documented and is favored among many in academia as well as in industry [1]. SCFDE, a PHY technique of similar complexity, has received much attention of late and has recently stimulated much "single-carrier vs multi-carrier" debate [2]. Both of these techniques utilize signal processing in the frequency domain to provide relatively low-complexity solutions to the problem of equalization. In [2], a comparison of these two technologies was conducted with a focus on single-antenna systems employed in fixed broadband wireless applications (IEEE 802.16) where the multipath spread of the channel is only a few non-zero discrete taps. However, to the best of our knowledge, an OFDM/SCFDE performance comparison has not been conducted for MIMO systems employed in wireless local area network (WLAN) applications where the effects of multipath propagation in the channel can be much greater.

In this paper, we present an investigation of the performance of several different MIMO-OFDM and MIMO-SCFDE systems in WLAN environments. In section II, an overview of the chosen MIMO-OFDM and MIMO-SCFDE systems is presented. In section III, the selected wireless channel models are discussed. The results that were obtained in this investigation are illustrated in section IV. Finally, conclusions are given in section V.

II. System Description

OFDM and SCFDE were applied to two MIMO baseband architectures: spatial multiplexing (SM) and space-time block coding (STBC). Two transmit antennas and two receive antennas were used in all systems. A generalized block diagram of the systems under investigation is shown in Figure 1.

The key architectural difference between a MIMO-OFDM system and a MIMO-SCFDE system, namely the order in which the IFFT operation is executed, is depicted in Figure 1. Other differences between the SCFDE and OFDM architectures include the implementation of the Viterbi decoder, the designs of the transmit and receive filters, and the structure of the frequency-domain equalizers. We address these dissimilarities below.

A. Viterbi Decoder Implementation

All MIMO architectures were simulated with and without a half-rate convolutional code with random bit interleaving following the encoder as depicted in Figure 1. The convolutional code used in this study is specified in [3], [4]. At the receiver,

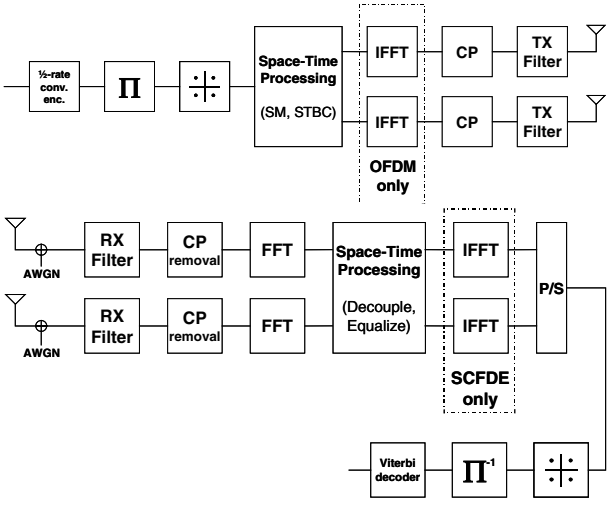

Fig. 1. Generalized block diagram of MIMO-OFDM and MIMO-SCFDE systems.

the equalized symbols were mapped to soft bits that were then passed through a soft-input hard-output Viterbi decoder as illustrated in Figure 1. The OFDM systems utilize channel state information (CSI) to weight the branch metrics, thus enhancing the performance of the Viterbi decoder. However, single-carrier systems are generally unable to utilize CSI in this fashion because the energy in each transmitted bit is spread across the entire bandwidth of the system. As a result, a standard soft-input hard-output Viterbi decoder was used in the SCFDE systems.

B. TX and RX Filter Design

In general, the transmit and receive filters in OFDM systems can be much tighter than those used in single-carrier systems. Consequently, we implemented root-raised-cosine filters with a roll-off factor of 0.4 at the transmitter and the receiver of each SCFDE system studied and root-raised-cosine filters with a roll-off factor of 0.025 at the transmitter and the receiver of each OFDM system [5]. Additionally, the bandwidth used by the simulated systems was kept as close to 20 MHz as possible. Therefore, to avoid the introduction of intersymbol interference (ISI) by the filters, the symbol periods for the OFDM and SCFDE systems were set equal to 50 ns and 70 ns, respectively. The full specifications of these filters are presented in Table I.

C. Equalizer Design

In each MIMO system, two factors affect the design of the frequency-domain equalizer: the PHY technique (i.e. OFDM or SCFDE) and the MIMO architecture (i.e. SM or STBC). Throughout this study, zero forcing (ZF) equalizers were implemented in the OFDM systems whereas minimum mean-squared error (MMSE) equalizers were employed in the SCFDE systems. Both of these common linear equalization techniques have similar complexity in the context of MIMO applications. Before discussing each system in turn, some notation is defined. The matrix $\mathbf{I}_q$ is the $q \times q$ identity matrix, $\mathbf{0}_q$ is the $q \times q$ zero matrix, $\otimes$ denotes the Kronecker product, and $(\cdot)_K$, $(\cdot)^*$, $(\cdot)^{\mathrm{T}}$, $(\cdot)^{\mathrm{H}}$, and $\mathrm{E}\{\cdot\}$ denote the modulo-K, complex conjugate, transpose, conjugate transpose, and expectation operations, respectively.

1) SM-OFDM: The SM-OFDM equalized symbol vector $\tilde{\mathbf{x}}$ is given by

$$\tilde{\mathbf{x}} = \mathbf{W}_{\mathbf{SM}} \left(\mathbf{\Lambda} \mathbf{x} + \eta \right) \tag{1}$$

where

$$\mathbf{\Lambda} = \begin{pmatrix} \widetilde{\mathbf{\Lambda}}_{1,1} & \dots & \widetilde{\mathbf{\Lambda}}_{1,n_t} \\ \vdots & \ddots & \vdots \\ \widetilde{\mathbf{\Lambda}}_{n_r,1} & \dots & \widetilde{\mathbf{\Lambda}}_{n_r,n_t} \end{pmatrix} \tag{2}$$

is the overall channel matrix of a system with n_t transmit antennas and n_r receive antennas and $\mathbf{W}_{\mathbf{SM}}$ is the ZF equalizer matrix. As previously mentioned, $n_t = n_r = 2$ in this study. The sub-matrix $\widetilde{\mathbf{\Lambda}}_{i,j}$ is a diagonal matrix defining the frequency response of all K subcarriers between the jth transmit antenna and the ith receive antenna. The vector $\mathbf{x}$ is a $2K \times 1$ vector of transmitted symbols and η is a $2K \times 1$ vector of white Gaussian noise samples. The ZF equalizer $\mathbf{W}_{\mathbf{SM}} = \mathbf{\Lambda}^{-1}$ removes the channel distortion from the received symbols at the expense of possibly enhancing the noise as seen in (1).

2) STBC-OFDM: For STBC-OFDM systems, equalization is performed after the received signals are combined [6]. If $\mathbf{s}$ is the stacked $2K \times 1$ vector of symbols after maximum ratio combining (MRC), the equalized symbol vector $\tilde{\mathbf{x}}$ is given by

$$\tilde{\mathbf{x}} = \mathbf{W}_{\mathbf{STBC}} \left(\mathbf{s} + \tilde{\eta} \right). \tag{3}$$

In (3), $\mathbf{W}_{\mathbf{STBC}} = \bar{\mathbf{\Lambda}}^{-1}$ is the ZF equalizer matrix where

$$\bar{\mathbf{\Lambda}} = diag \left\{ \sum_{i,j} \left(h^{(1)}_{i,j,1} \right)^2, \dots, \sum_{i,j} \left(h^{(p)}_{i,j,k} \right)^2 \right\}$$

is a diagonal matrix and $h^{(p)}_{i,j,k}$ is the channel gain between the jth transmit antenna and the ith receive antenna on subcarrier k for the pth MRC signal. The vector $\tilde{\eta}$ is the noise after MRC.

3) SM-SCFDE: For SM-SCFDE systems, the vector $\tilde{\mathbf{x}}$ of equalized symbols at both receive antennas is given by

$$\tilde{\mathbf{x}} = \mathbf{D}_{\mathbf{F}}^{-1} \overline{\mathbf{W}}_{\mathbf{SM}} \left(\mathbf{\Lambda} \mathbf{D}_{\mathbf{F}} \mathbf{x} + \mathbf{D}_{\mathbf{F}} \eta \right) \tag{4}$$

where $\mathbf{D}_{\mathbf{F}} = \mathbf{I}_2 \otimes \mathbf{F}$. The matrix $\mathbf{F}$ is the $K \times K$ FFT matrix where K is the length of each transmitted block in the SCFDE system. In (4), $\overline{\mathbf{W}}_{\mathbf{SM}}$ is the MMSE equalizer matrix defined in [7] and reproduced below for convenience.

$$\overline{\mathbf{W}}_{\mathbf{SM}} = \mathbf{\Lambda}^{\mathrm{H}} \left(\mathbf{\Lambda} \mathbf{\Lambda}^{\mathrm{H}} + \frac{\sigma_\eta^2}{\sigma_x^2} \mathbf{I}_{2K} \right)^{-1}. \tag{5}$$

The quantity σ_η^2 is the total variance of the complex Gaussian noise process at one receive antenna, σ_x^2 is the total power of the complex transmitted signal from one transmit antenna, and $\mathbf{\Lambda}$ is defined in (2). As observed in (4), the equalizer spans both receiver branches to separate the transmitted symbol streams and equalize the received symbols simultaneously.

4) STBC-SCFDE: The MMSE equalizer used in the STBC-SCFDE systems, first discussed in [8], is different from that employed in the SM-SCFDE systems in that the decoupling and equalization processes are performed separately. To illustrate, let $\mathbf{x}^{(1)}_\ell$ and $\mathbf{x}^{(2)}_\ell$ be the two $K \times 1$ symbol vectors transmitted from the first and second antennas respectively at time ℓ. Then the two vectors transmitted at time $\ell+1$, directly after the first two vectors, are defined by

$$\begin{aligned} \mathbf{x}^{(1)}_{\ell+1}(k) &= -\mathbf{x}^{*(2)}_\ell \left((-k)_K \right) \\ \mathbf{x}^{(2)}_{\ell+1}(k) &= \mathbf{x}^{*(1)}_\ell \left((-k)_K \right) \end{aligned}$$

for $k = 0, 1, \dots, K-1$. At the receiver, the vectors corresponding to those transmitted during the $(\ell+1)$th time slot are conjugated, after which each received vector is transformed into the frequency domain and MRC is implemented to decouple the transmitted sequences. The resulting length-$2K$ vector of symbols prior to equalization is given by

$$\mathbf{Y} = \sum_{i=1}^{2} \widehat{\mathbf{\Lambda}}^{\mathrm{H}(i)} \left(\widehat{\mathbf{\Lambda}}^{(i)} \mathbf{D}_{\mathbf{F}} \mathbf{x} + \mathbf{D}_{\mathbf{F}} \eta^{(i)} \right) \tag{6}$$

where

$$\widehat{\mathbf{\Lambda}}^{(i)} = \begin{pmatrix} \widetilde{\mathbf{\Lambda}}_{i,1} & \widetilde{\mathbf{\Lambda}}_{i,2} \\ \widetilde{\mathbf{\Lambda}}^{*}_{i,2} & -\widetilde{\mathbf{\Lambda}}^{*}_{i,1} \end{pmatrix},$$

$\widetilde{\mathbf{\Lambda}}_{i,j}$ is defined in (2), $\mathbf{x} = (\mathbf{x}_{\ell}^{\mathrm{T}(1)}, \mathbf{x}_{\ell}^{\mathrm{T}(2)})^{\mathrm{T}}$, and $\eta^{(i)}$ represents the noise contribution from the ith receive antenna. The sequence $\mathbf{Y}$ is then passed through an MMSE equalizer. The equalizer matrix $\overline{\mathbf{W}}_{\mathbf{STBC}}$ for this system is obtained by solving the equation

$$\overline{\mathbf{W}}_{\mathbf{STBC}} = \arg\min_{\mathbf{W}} \mathrm{E}\left\{ |\mathbf{x} - \tilde{\mathbf{x}}|^2 \right\} \tag{7}$$

where $\tilde{\mathbf{x}} = \mathbf{D}_{\mathbf{F}}^{-1}\mathbf{W}\mathbf{Y}$ represents the equalized symbols in the time domain. It can be shown that the solution to (7) is [6], [8]

$$\overline{\mathbf{W}}_{\mathbf{STBC}} = \left(\breve{\mathbf{\Lambda}} + \frac{\sigma_{\eta}^2}{\sigma_{x}^2} \mathbf{I}_{2K} \right)^{-1} \tag{8}$$

where

$$\breve{\mathbf{\Lambda}} = \begin{pmatrix} \sum_{i=1}^{2}\sum_{j=1}^{2} \left| \widetilde{\mathbf{\Lambda}}_{i,j} \right|^2 & \mathbf{0}_K \\ \mathbf{0}_K & \sum_{i=1}^{2}\sum_{j=1}^{2} \left| \widetilde{\mathbf{\Lambda}}_{i,j} \right|^2 \end{pmatrix}. \tag{9}$$

III. Channel Description

In [9], five different indoor WLAN channel models are described. For this study, the channel models with the shortest and the longest RMS delay spreads were chosen. The ETSI A model corresponds to a typical office environment and has an RMS delay spread of 50 ns, whereas the ETSI E model corresponds to a typical large open space environment with an RMS delay spread of 250 ns. Both of these channels represent non-line-of-sight (NLOS) conditions in their respective environments. In the simulations, statistically independent Rayleigh fading channel realizations were generated, and the receiver was assumed to have complete knowledge of the channel. Although these models are specified for 100 MHz bandwidth, the filters discussed in section II-B were employed to give an RF bandwidth of 20 MHz.

IV. Simulation Results

To provide a fair comparison, several system parameters were held constant in the simulations. A complete list of the simulation parameters is given in Table I. It is important to note that the number of bits in a packet specified in Table I includes six tail bits used to return the encoder to the zero state for the systems implementing the convolutional code.

As metrics of performance, packet error rate (PER) and throughput were used. To simulate the PER of a system, one packet was transmitted for each independent channel realization. The transmission of one packet was assumed to be well within the coherence time of the channel. The PERs of systems employing QPSK and 16-QAM in the ETSI A channel are shown in Figure 2. Likewise, the PERs of systems employing QPSK and 16-QAM in the ETSI E channel are shown in Figure 3. Figures 4 and 5 show the throughputs of

TABLE I

Simulation parameters.

	SCFDE Parameters	**OFDM Parameters**
Bandwidth	20 MHz	20.5 MHz
Modulation	QPSK & 16-QAM	QPSK & 16-QAM
Channels simulated	ETSI A & E	ETSI A & E
Convolutional encoder	(2,1,6) [3], [4]	(2,1,6) [3], [4]
Viterbi decoder	soft-input hard-output (standard)	soft-input hard-output (weighted metrics)
Equalization	MMSE	ZF
Bits per packet	1024	1024
No. of subcarriers (symbols per block)	64	64
TX filter	RRC	RRC
Sample rate	7 samples/symbol	5 samples/symbol
Filter span	10 symbols	10 symbols
Roll-off factor	0.4	0.025 [5]
RX filter	RRC	RRC
Sample rate	7 samples/symbol	5 samples/symbol
Filter span	10 symbols	10 symbols
Roll-off factor	0.4	0.025 [5]
Symbol period	70 ns	50 ns
Cyclic prefix	12 sym. $\rightleftharpoons$ 840 ns	17 sym. $\rightleftharpoons$ 850 ns

the simulated systems in the ETSI A and ETSI E channels, respectively. In Figures 2 through 5, *cd* signifies a system in which the convolutional code is employed, *uncd* signifies a system that does not utilize the code; curves related to SCFDE systems are solid lines, and curves related to OFDM systems are dot-dashed lines.

A. PER Analysis

The graphs presented in Figures 2 and 3 show a number of interesting trends. Firstly, as expected, the uncoded SM-OFDM systems perform extremely poorly and are, in general, outperformed by the SM-SCFDE systems. This is most obvious in Figure 2(a) where the SNR gain of the uncoded SM-SCFDE system is about 10 dB at a PER of 0.3. Secondly, the best PER performance is achieved by concatenating a channel code with STBC. This is also expected since this arrangement exploits spatial diversity and coding. Furthermore, the performance difference between the OFDM and SCFDE system with this particular architecture is at most 0.5 dB.

It is interesting to note that results published in [2] for single-input single-output (SISO) systems with linear equalization show that for a sufficiently strong channel code, OFDM systems outperform SCFDE systems. In the MIMO case, however, this trend appears to be reversed as shown by the coded SM and uncoded STBC curves in Figures 2 and 3. An exception to the trend is seen in Figure 2(b), where it is shown that the SM-SCFDE system performs approximately 2 dB worse than the SM-OFDM system in the ETSI A channel when a 16-QAM constellation is used. This behavior is most likely due to the limitations of MMSE equalization when dense signal constellations are used. Identical behavior is not observed for transmissions in the ETSI E channel

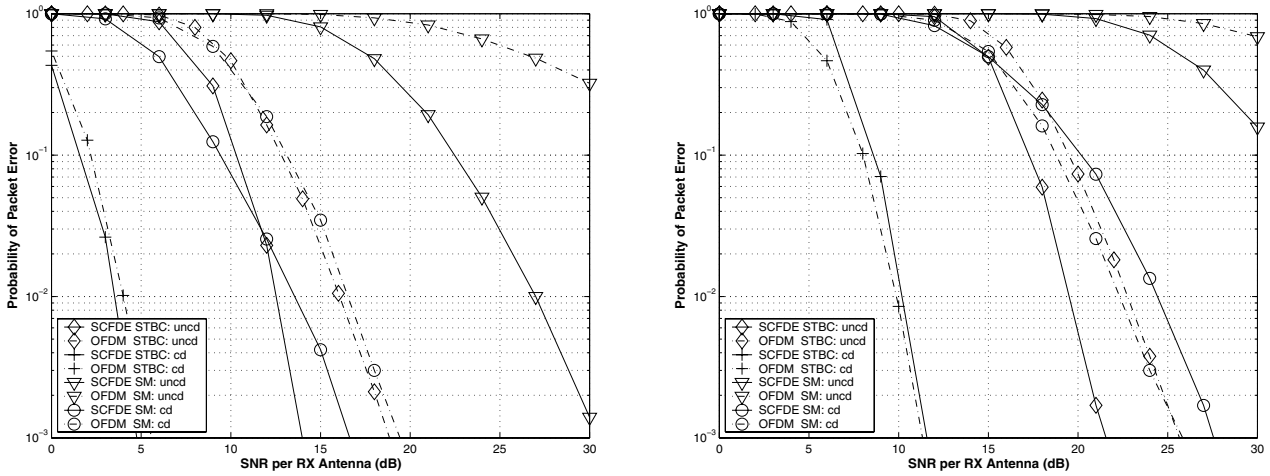

(a) QPSK (b) 16-QAM

Fig. 2. Packet error rates for STBC and SM systems in the ETSI A channel ($n_t = n_r = 2$).

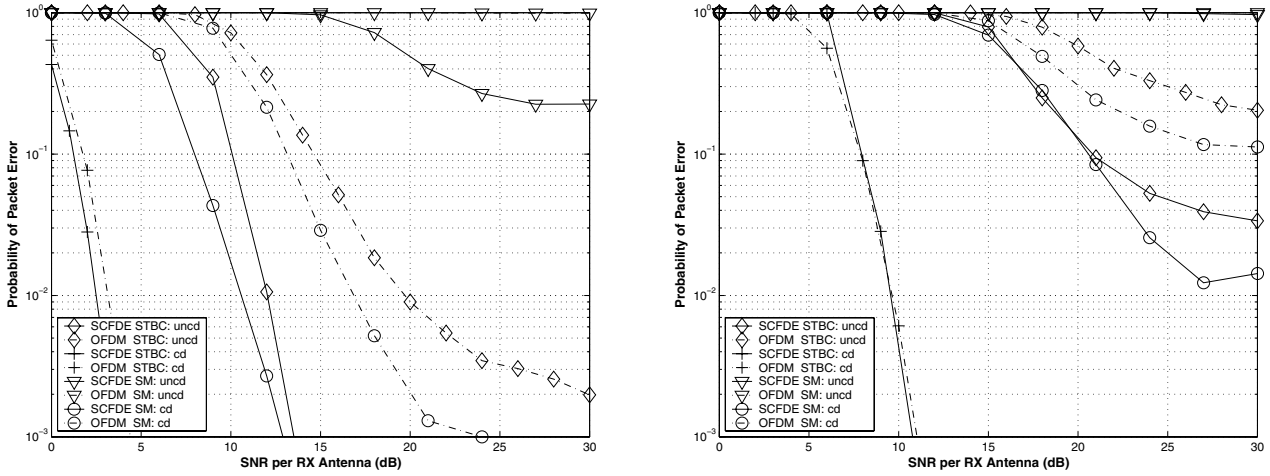

(a) QPSK (b) 16-QAM

Fig. 3. Packet error rates for STBC and SM systems in the ETSI E channel ($n_t = n_r = 2$).

due to SCFDE's efficient utilization of frequency diversity and OFDM's sensitivity to the loss of orthogonality between subcarriers, which is caused by an insufficient cyclic prefix.

The results also show the trade-off between SM and STBC schemes for wideband systems. For example, in the ETSI A channel, the coded SM and uncoded STBC-OFDM systems perform almost identically as shown in Figure 2(a). However, in the ETSI E channel, the SM-OFDM system outperforms the STBC-OFDM system in Figure 3(a) by approximately 3 dB at a PER of 0.01. A similar trend can be seen for the same systems with 16-QAM modulation in Figures 2(b) and 3(b). These trends imply that the exploitation of frequency diversity can potentially provide better performance gains for MIMO-OFDM systems than the utilization of spatial diversity alone. In practical terms this means that importance should be placed on the type of channel code employed over the type of diversity scheme used. Frequency diversity can be exploited further by increasing the number of subcarriers used in the system, which decreases the subcarrier spacing thus causing small perturbations in the channel to become significant. The practical trade-off here is that the OFDM system becomes more sensitive to synchronization errors and imperfect channel knowledge as the number of subcarriers increase.

In the SCFDE systems, the trade-off between SM and STBC is most obvious in the ETSI A channel where the coded SM-SCFDE systems perform better at low SNR while the STBC-SCFDE systems perform better at high SNR as shown in Figures 2(a) and 2(b). The crossover occurs at an SNR of approximately 12 dB (PER = 0.025) for the QPSK modulation and at an SNR of 15 dB (PER = 0.5) for 16-QAM, which suggests that spatial diversity exploited through the STBC significantly aids the detection process in a channel with low frequency selectivity such as the ETSI A channel. Additionally, in rich scattering environments, SCFDE

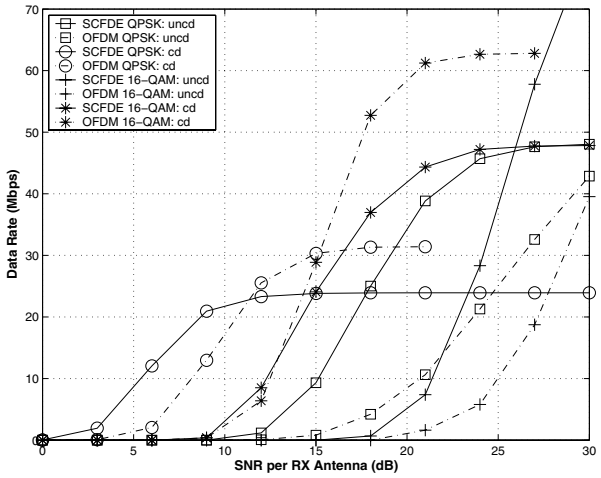

(a) SM

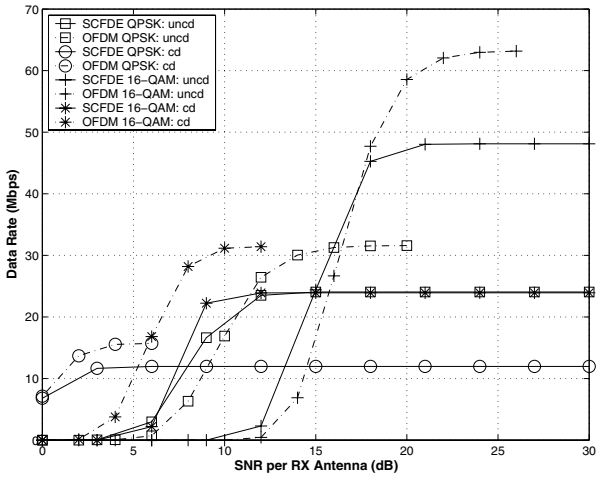

(b) STBC

Fig. 4. Throughput for systems in ETSI A channel.

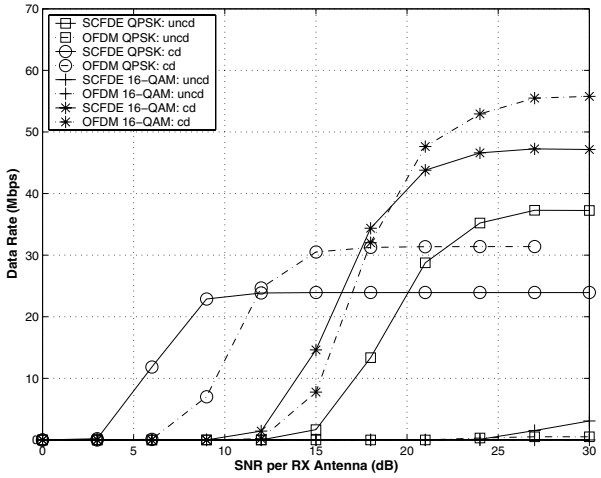

(a) SM

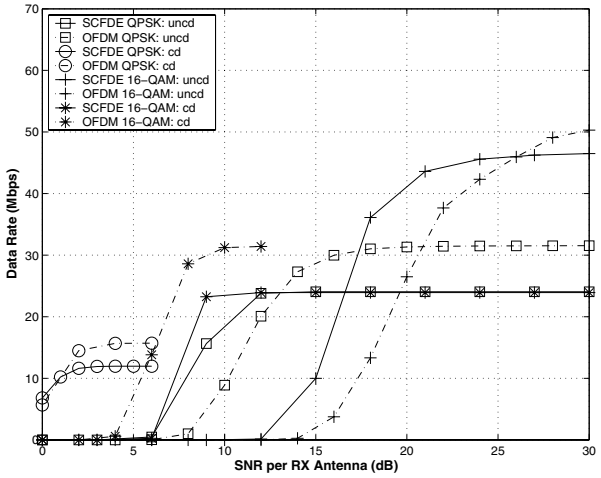

(b) STBC

Fig. 5. Throughput for systems in ETSI E channel.

efficiently exploits frequency diversity, which leads to better overall performance. This is clearly depicted in Figures 3(a) and 3(b), where the coded SM-SCFDE systems perform better than the uncoded STBC-SCFDE systems.

B. Throughput Analysis

The throughput for each simulated system was calculated as a function of the SNR from the following equation.

$$D(\text{SNR}) = \frac{2mKR\,(N-v)}{NT_s\,(K+Q)\,(1+\mu)}\,(1-\wp\,(\text{SNR})) \qquad (10)$$

where m is the number of bits per symbol, R is the code rate, N is the total number of bits in a packet prior to encoding, v is the number of tail bits in a packet, T_s is the symbol period, Q is the number of symbols used for a cyclic prefix in each block, μ is equal to one if the system utilizes STBC and zero otherwise, and $\wp\,(\gamma)$ is the PER as a function of SNR.

Figures 4 and 5 illustrate the effect the high filter roll-off factor has on the single-carrier systems. Indeed, the OFDM systems generally provide higher throughput than the SCFDE systems. It is interesting to note, however, that advantages can be gained through the use of a hybrid SCFDE-OFDM link adaptive system, especially for SM architectures. As shown in Figures 4(a) and 5(a), coded SCFDE systems provide the highest throughput at low SNR for SM architectures. Furthermore, uncoded SCFDE systems employing 16-QAM give the highest throughput at high SNR for SM systems in the ETSI A channel as illustrated in Figure 4(a). It is also important to note that for mid-range SNR, the single-carrier STBC system is capable of a higher throughput than the OFDM system in the ETSI E channel as illustrated in 5(b).

V. Conclusions

In this study, several different MIMO-SCFDE and MIMO-OFDM systems were compared in terms of PER and throughput. The results obtained in this investigation suggest that designing a MIMO-OFDM system to exploit frequency diversity through the use of a channel code and interleaving tends to give better performance than optimizing for spatial diversity through the use of STBC. Similarly, SM-SCFDE systems employing linear MMSE equalization and a channel code perform relatively well in rich scattering environments; however, optimizing for spatial diversity via STBC can improve the performance of SCFDE systems in channels with low frequency selectivity. Additionally, unlike in the SISO case, MIMO-SCFDE generally performs better than MIMO-OFDM in terms of PER. It was also shown that the throughput of MIMO-SCFDE systems will inevitably suffer from the tight constraints placed on the transmit and receive filters unless bandwidth restrictions are relaxed.

Acknowledgment

The authors would like to thank Toshiba TRL Bristol for financially supporting this work and are particularly grateful for the insight provided by Dr. M. Sandell, Dr. M. Yee, Dr. S. Parker, and Dr. Y. Sun. The authors are also indebted to Dr. R. Piechocki for his participation in numerous technical discussions.

References

[1] Z. Wang and G. B. Giannakis, "Wireless multicarrier communications: where Fourier meets Shannon," *IEEE Signal Processing Magazine*, pp. 29–47, May 2000.

[2] D. Falconer, S. L. Ariyavisitakul, A. Benyamin-Seeyar, and B. Eidson, "Frequency domain equalization for single-carrier broadband wireless systems," *IEEE Communications Magazine*, pp. 58–66, April 2002.

[3] *Broadband Radio Access Networks (BRAN); HIPERLAN Type 2; Physical (PHY) layer*, European Telecommunications Standards Institute, 2000.

[4] *Supplement to IEEE standard for information technology - telecommunications and information exchange between systems - local and metropolitan area networks - specific requirements. Part 11: wireless LAN Medium Access Control (MAC) and Physical Layer (PHY)*, IEEE Std 802.11a, 1999.

[5] R. van Nee and R. Prasad, *OFDM for Wireless Multimedia Communications*, 1st ed. Boston: Artech House, 2000.

[6] S. M. Alamouti, "A simple transmit diversity technique for wireless communications," *IEEE Journal on Selected Areas in Communications*, vol. 16, no. 8, pp. 1451–1458, October 1998.

[7] J. P. Coon and M. A. Beach, "An investigation of MIMO single-carrier frequency-domain MMSE equalization," *London Communications Symposium*, pp. 237–240, 2002.

[8] N. Al-Dhahir, "Single-carrier frequency-domain equalization for space-time block-coded transmissions over frequency-selective fading channels," *IEEE Communications Letters*, vol. 5, no. 7, pp. 304–306, July 2001.

[9] *Channel Models for HIPERLAN/2 in Different Indoor Scenarios*, European Telecommunications Standards Institute, 1998.